Available online at www.sciencedirect.com
ScienceDirect
C. R. Geoscience 340 (2008) 127–138
COMPTES RENDUS GEOSCIENCE
http://france.elsevier.com/direct/CRAS2A/

Tectonics

Discovery of high-pressure granulite-facies metamorphism in northern Vietnam: Constraints on the Permo-Triassic Indochinese continental collision tectonics

Nobuhiko Nakano [a,*], Yasuhito Osanai [a], Nguyen Thi Minh [a], Tomoharu Miyamoto [b], Yasutaka Hayasaka [c], Masaaki Owada [d]

[a] *Division of Evolution of Earth Environments, Faculty of Social and Cultural Studies, Kyushu University, 4-2-1 Ropponmatsu, Chuo-ku, Fukuoka 810-8560, Japan*
[b] *Department of Earth and Planetary Sciences, Kyushu University, Fukuoka 812-8581, Japan*
[c] *Department of Earth and Planetary Systems Science, Hiroshima University, Higashi-Hiroshima 739-8526, Japan*
[d] *Division of Earth Sciences, Graduate school of Science and Technology, Yamaguchi University, Yamaguchi 753–8511, Japan*

Received 2 July 2007; accepted after revision 29 October 2007
Available online 26 December 2007

Written on invitation of the Editorial Board

Abstract

High-pressure mafic granulites containing granoblastic garnet, quartz, and minor hornblende have been found from the Song Ma Suture zone in northern Vietnam, regarded as a microcontinental boundary between the South China and Indochina blocks. Fine-grained symplectite formed during the decompression stage is developed in the granulite and is divided into orthopyroxene + -plagioclase and orthopyroxene + clinopyroxene + plagioclase ± hornblende. The former replaces garnet and the latter is regarded as a breakdown of sodic clinopyroxene. Detailed observation and careful data selection revealed that the high-Mg and low-Ca garnet should be in equilibrium with the precursor sodic clinopyroxene, and the pair indicates high-temperature and -pressure conditions (910–930 °C at 1.9–2.0 GPa). Although we could not obtain quantitative age data from the high-pressure granulite, the U–Th–Pb age (233 ± 5 Ma) of pelitic gneiss strongly suggests a Middle to Early Triassic metamorphic event. If the age indicates the timing of the high-pressure granulite-facies metamorphism, it might be related to a continental collision setting by following crustal subduction. According to the metamorphic signatures, north to central Vietnam may be regarded as an orogenic belt formed by the micro-continental collision between the South China and Indochina cratons. ***To cite this article: N. Nakano et al., C. R. Geoscience 340 (2007).***

Résumé

Découverte d'un métamorphisme granulitique de haute-pression dans le Nord du Vietnam : implications sur la tectonique de collision continentale de l'Indochine au Permo-Trias. Des granulites basiques de haute pression, contenant grenat granoblastique, quartz et une faible proportion de hornblende, ont été découvertes dans la partie nord du Vietnam, au niveau de la zone de suture de Song Ma, considérée comme formant la frontière des microblocs continentaux de Chine du Sud et d'Indochine. Une symplectique à grain fin, formée lors de la période de décompression, s'est développée dans la granulite, se subdivisant en

* Corresponding author.
E-mail address: n-nakano@scs.kyushu-u.ac.jp (N. Nakano).

1631-0713/$ – see front matter © 2007 Académie des sciences. Published by Elsevier Masson SAS. All rights reserved.
doi:10.1016/j.crte.2007.10.013

orthopyroxène + plagioclase et orthopyroxène + clinopyroxène + plagioclase ± hornblende. La première phase minérale remplace le grenat, alors que la dernière est considérée comme la dégradation du clinopyroxène sodique. Une observation de détail et une sélection attentive des données révèlent que le grenat à haute teneur en Mg et à faible teneur en Ca devrait être en équilibre avec le clinopyroxène sodique précurseur ; ces deux éléments indiquent des conditions de haute température et de haute pression (910–930 °C à 1,9–2,0 GPa). Bien que nous n'ayons pu obtenir de données quantitatives d'âge pour la granulite de haute pression, un âge U–Th–Pb (233 ± 5 Ma), obtenu dans les gneiss pélitiques, suggère fortement qu'il s'agit d'un événement métamorphique du Trias inférieur à moyen. Si cet âge représente effectivement celui du métamorphisme granulitique de haute pression, alors il pourrait résulter d'un contexte de collision continentale faisant suite à une subduction crustale. Compte tenu des signatures métamorphiques, le segment allant du Centre au Nord du Vietnam peut être considéré comme une ceinture orogénique formée par la collision entre les microcontinents de Chine du Sud et du Vietnam. ***Pour citer cet article : N. Nakano et al., C. R. Geoscience 340 (2007).***

Keywords: High-pressure granulite; Triassic; Continental collision; Song Ma Suture zone; Vietnam; Indochina

Mots clés : Granulite de haute pression ; Trias ; Collision continentale ; Zone de suture de Song Ma ; Vietnam ; Indochine

1. Introduction

High-pressure granulite facies, defined by several experimental studies [9,11,14], are characterised by the presence of garnet in orthopyroxene-bearing mafic rocks. The upper pressure limit of a high-pressure granulite assemblage is characteristically specified by the lack of plagioclase and orthopyroxene. This means that an assemblage of garnet + clinopyroxene + quartz is one of the characteristics of the eclogite facies [3]. According to [27], high-pressure granulites can be subdivided into three types: high- to ultrahigh-temperature, moderate-temperature, and xenolithic types. The former two types are formed at subduction and continental collision zones [27]. Therefore, the presence of high-pressure granulites in the regional metamorphic belt (terrane) is important in defining past plate convergence zones, and their pressure/temperature/time conditions are indicators in understanding the history of the crustal collision process.

The Asian continent is considered to have amalgamated a large number of microcontinents [22]. Indochina has been regarded as an assemblage of three major microcontinental blocks (Fig. 1A), namely, the South China, Indochina and Shan-Thai blocks (Fig. 1A; [10]). The main problems in the geology of this region are the position of the real continental boundary, and when these microcontinents collided with each other. The boundary between the South China and Indochina cratons has been considered the Song Ma Suture zone [22] or the Red River Shear zone [38], and the collision occurred in the Permo-Triassic [16] or before the Devonian [22]. In this study, we used a metamorphic petrology approach to understand the tectonic setting of the Indochina block; in particular, the discovery of high-pressure granulite from the Song Ma Suture zone in northern Vietnam and its pressure/temperature conditions are reported. Finally, their geological significances are argued.

2. Geological outline

The Song Ma Suture zone is situated in northern to northwestern Vietnam (partly in northeastern Laos). Along the suture zone, metamorphic rocks are widely distributed and form a metamorphic belt (Fig. 1B). Several serpentinite lenses are occasionally exposed within the metamorphic belt, and have been regarded as relicts of the former Palaeotethyan lithosphere [13]. The metamorphic rocks have been divided into the Nam Co and the Nam Su Lu formations based on the metamorphic grade; the former is of lower grade than the latter [4]. Between them, later granitoids are widely distributed (Fig. 1C). In the Nam Co Formation, pelitic schists such as muscovite and garnet-phengite schists are dominant, and mafic and calc-silicate rocks are generally observed as blocks. In the Nam Su Lu Formation, mafic rocks are well distributed. Amphibolite and garnet amphibolite are major lithologies, and pelitic gneisses such as garnet–biotite and garnet–sillimanite–biotite gneisses are often intercalated with them. Kyanite and andalusite, which were often observed in pelitic rocks from the Nam Co formation, have not been observed in those from the Nam Su Lu Formation.

High-pressure granulite (garnetclinopyroxene granulite), the focus of this study, was collected as a boulder along the Nam Ma River in the Nam Su Lu Formation, where the upstream limits of the rivers are also inside the formation (Fig. 1C) and there are no metamorphic terranes in the upstream. Because we have never seen the metamorphic blocks in igneous rocks (as xenolith)

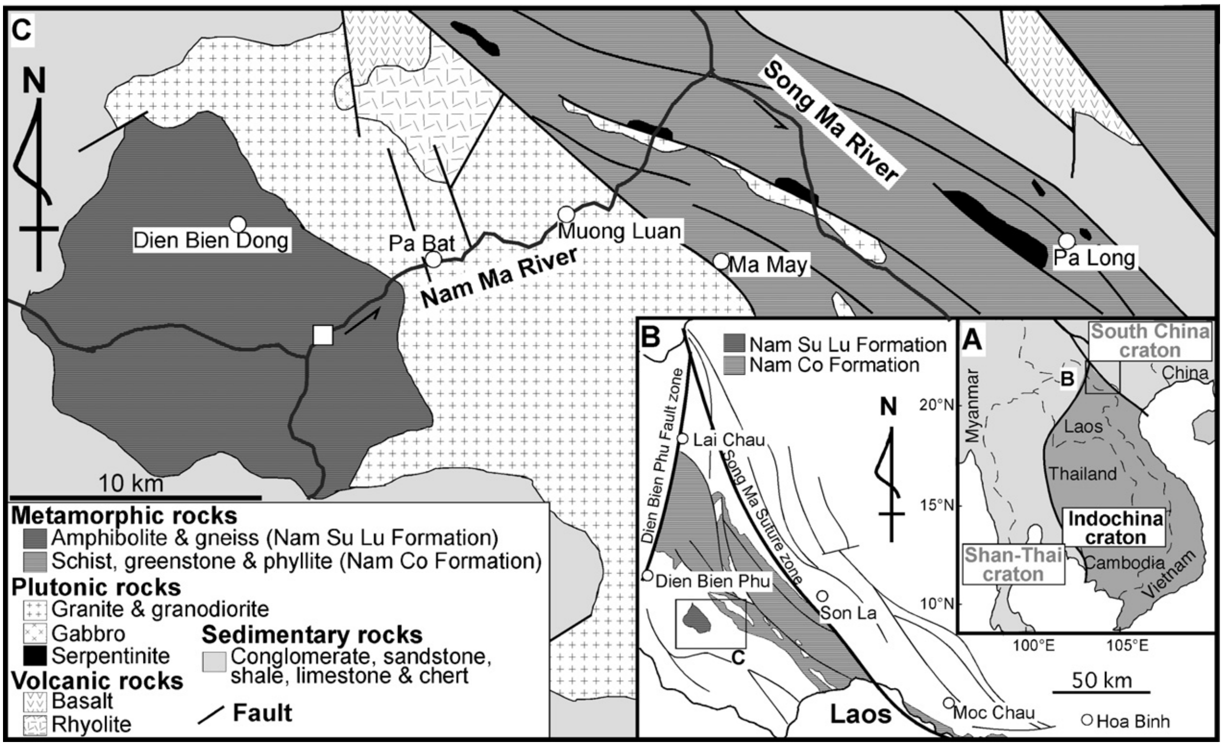

Fig. 1. Distribution of micro-continental blocks in the Indochina [9] (**A**), division of metamorphic rocks (**B**) and simplified geological map in the studied area [4] (**C**). A square indicates locality of high-pressure granulite studied. Arrows shown along rivers in Fig. 1C indicate directions of river flow.

Fig. 1. Distribution des microblocs continentaux dans la péninsule Indochinoise (9) (**A**), subdivisions des roches métamorphiques (**B**) et carte géologique simplifiée de la zone étudiée (4) (**C**). Un carré indique la localisation de la granulite étudiée. Les flèches au long des rivières sur la Fig. 1C indiquent la direction du courant.

and in conglomerate (as pebble) from the studied area, the boulder might be derived from the Nam Su Lu Formation itself.

3. Petrography of high-pressure granulite

The high-pressure granulite (garnetclinopyroxene granulite) contains coarse grains of garnet and quartz with a minor amount of hornblende, ilmenite, and rutile (Fig. 2A). Orthopyroxene + clinopyroxene + plagioclase ± hornblende ± quartz symplectite is widely present in the matrix (Fig. 2A). The garnet is replaced with orthopyroxene + plagioclase coronas and its grain size varies (Fig. 2A). A thin orthopyroxene moat is present on the clinopyroxene and quartz side of the corona (Fig. 2A and B). The corona and moat suggest that the original garnet was subhedral to euhedral in shape and up to 2 mm in diameter (Fig. 2A and B). The garnet contains several mineral inclusions of amphibole (pargasite–tschermakite), ilmenite, rutile, apatite, and quartz. Hornblende is observed as subhedral grains and is mostly brownish green to brown in colour (Fig. 2A).

The orthopyroxene + clinopyroxene + plagioclase ± hornblende ± quartz symplectite is generally observed as an interstitial material (Fig. 2A). The symplectite sometimes has the euhedral shape of the original mineral crystal (Fig. 2B), suggesting that the symplectite was formed by breakdown of a single mineral phase. Some relatively large grains of quartz are also observed in the symplectite (Fig. 2C). Orthopyroxene in the symplectite has a subhedral shape and is always associated with symplectitic plagioclase (Fig. 2D). Orthopyroxene and plagioclase are not observed as individual grains in the matrix, and they always appear as symplectitic materials (Fig. 2A–D).

4. Mineral chemistry

The mineral chemistry was analysed using a scanning electron microscope with an energy-dispersive spectrometry system (JEOL JED2140-JSM 5301S) at the Kyushu University. The quantitative analyses of rock-forming minerals were performed with 15 kV accelerating voltage, using data processing with the

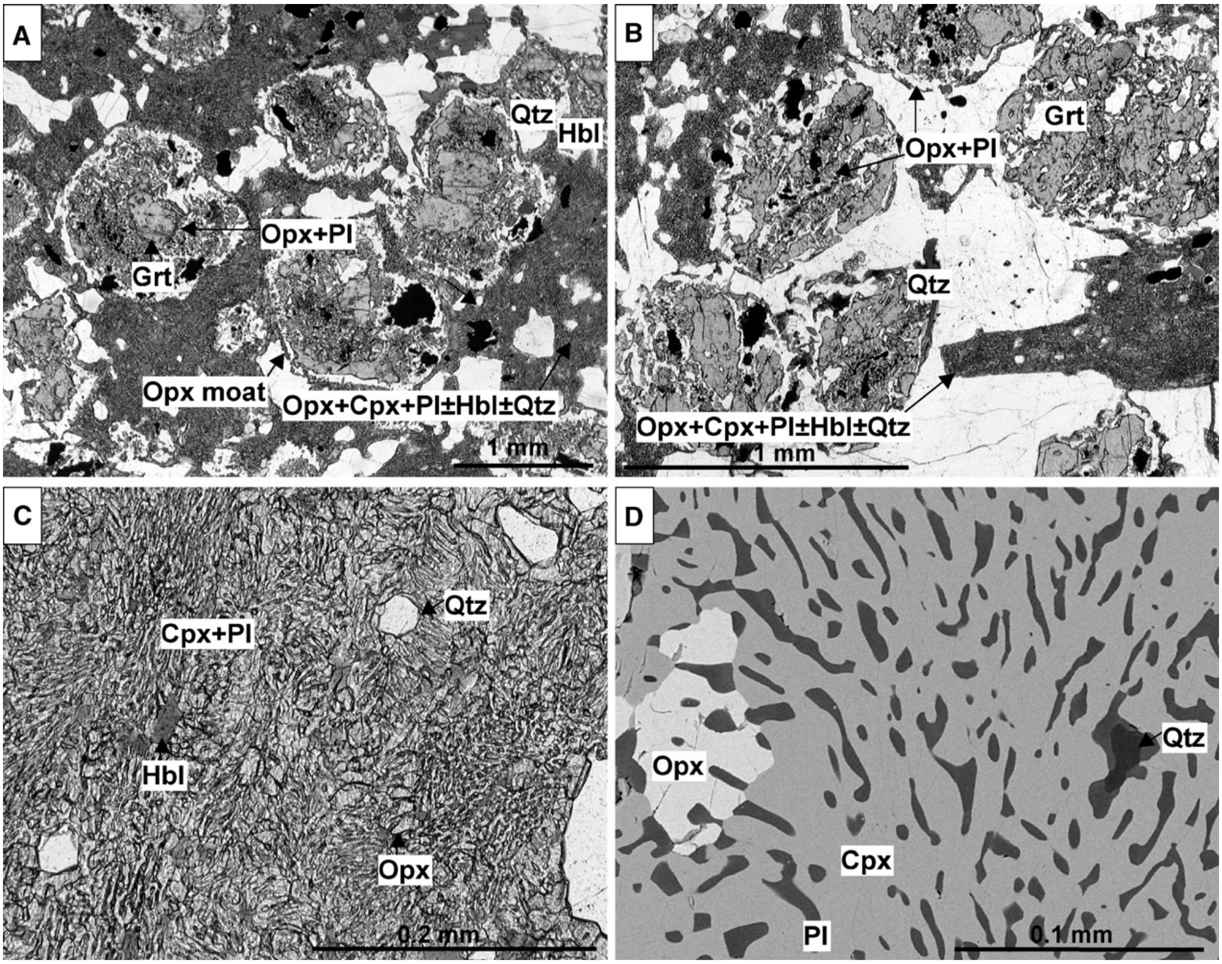

Fig. 2. Photomicrographs and a backscattered image of high-pressure granulite. **A–B**: Granoblastic garnet, hornblende and quartz with orthopyroxene + plagioclase corona around garnet and orthopyroxene + clinopyroxene + plagioclase ± hornblende ± quartz symplectite. Garnet is of euhedral shape before the formation of the orthopyroxene + plagioclase corona. Note that orthopyroxene + clinopyroxene + plagioclase ± hornblende ± quartz symplectite was formed by the breakdown of a single phase sometimes showing a euhedral shape. **C–D**: Orthopyroxene + clinopyroxene + plagioclase ± hornblende ± quartz symplectite. Quartz is observed as relatively large grains.

Fig. 2. Microphotographies et image rétrodiffusée de la granulite de haute pression. **A–B** : Grenat granoblastique, hornblende et quartz avec orthopyroxène + couronne de plagioclase autour du grenat et de l'orthopyroxène + clinopyroxène + plagioclase ± hornblende ± quartz symplectite. Le grenat est de forme euhédrale avant la formation de l'orthopyroxène + couronne de plagioclase. Noter que l'ensemble orthopyroxène + clinopyroxène + plagioclase ± hornblende ± quartz symplectite a été formé par la déstabilisation d'une phase unique montrant quelquefois une forme euhédrale. **C–D** : orthopyroxène + clinopyroxène + plagioclase ± hornblende ± quartz symplectite. Le quartz est présent sous la forme de grains relativement grands.

ZAF correction program. Natural mineral samples (ASTIMEX-MINM-53) were used as standards for the analyses. Representative analyses are shown in Tables 1 and 2.

4.1. Garnet

The chemical composition of garnet in the high-pressure granulite shows almandine, pyrope and grossular components. A small amount of spessartine component (less than Sps_4) is observed in the outer thin rim of the garnet. The core of the garnets can be grouped into two types based on their chemical compositions: high-Mg and low-Ca (garnet 1: $Alm_{58–62}Prp_{16–21}Grs_{19–24}Sps_{0–2}$) and low-Mg and high-Ca contents (garnet 2: $Alm_{56–62}Prp_{9–13}Grs_{25–32}Sps_{0–2}$) (Fig. 3). The mantle of garnet 1 is at the mid-position of both garnet cores, or sometimes shows a composition similar to that of the core of garnet 2 (Fig. 3). On the other hand, garnet 2 has a homogeneous composition, except in its outer thin rim

Table 1
Representative garnet analyses of Grt-Cpx granulite

Tableau 1
Analyses représentatives de grenat dans la granulite à Grt-Cpx

Type	Grtl						Grt2					
	Core	Core	Mantle	Mantle	Rim	Rim	Core	Core	Mantle	Mantle	Rim	Rim
SiO_2	38.78	38.44	38.81	38.11	37.81	37.96	38.66	38.52	38.22	38.15	38.38	37.59
TiO_2	0.11	0.26	0.15	0.23	0.00	0.19	0.00	0.29	0.37	0.00	0.06	0.00
$A1_2O_3$	21.39	21.14	21.77	21.03	21.15	20.91	21.71	20.94	20.92	21.56	21.00	21.23
$Cr2O_3$	0.40	0.00	0.08	0.00	0.00	0.00	0.00	0.00	0.18	0.00	0.28	0.00
FeO	27.29	28.11	27.59	26.97	28.84	28.04	27.32	26.99	26.77	26.31	30.41	28.96
MnO	0.77	0.54	0.41	0.42	2.20	1.25	0.60	0.81	0.22	0.31	1.27	0.91
MgO	4.45	4.50	3.00	4.09	1.88	2.39	3.21	2.46	2.74	3.07	2.24	2.03
CaO	7.98	7.47	10.03	8.60	8.15	9.45	9.88	11.40	10.92	10.49	8.19	8.12
Na_2O	0.00	0.00	0.00	0.00	0.00	0.00	0.00	0.00	0.00	0.00	0.00	0.18
K_2O	0.00	0.00	0.00	0.00	0.00	0.00	0.00	0.00	0.00	0.00	0.00	0.00
Total	101.17	100.46	101.84	99.45	100.03	100.19	101.38	101.41	100.34	99.89	101.83	99.02
O	12	12	12	12	12	12	12	12	12	12	12	12
Si	3.009	3.009	3.003	3.009	3.014	3.009	3.004	3.009	3.006	3.002	3.012	3.015
Ti	0.006	0.015	0.009	0.014	0.000	0.011	0.000	0.017	0.022	0.000	0.004	0.000
Al	1.956	1.950	1.986	1.957	1.987	1.954	1.988	1.928	1.940	2.000	1.942	2.007
Cr	0.025	0.000	0.005	0.000	0.000	0.000	0.000	0.000	0.011	0.000	0.017	0.000
Fe	1.771	1.840	1.786	1.781	1.923	1.859	1.775	1.763	1.761	1.731	1.996	1.943
Mn	0.051	0.036	0.027	0.028	0.149	0.084	0.039	0.054	0.015	0.021	0.084	0.062
Mg	0.515	0.525	0.346	0.481	0.223	0.282	0.372	0.286	0.321	0.360	0.262	0.243
Ca	0.663	0.626	0.832	0.728	0.696	0.803	0.823	0.954	0.920	0.884	0.689	0.698
Na	0.000	0.000	0.000	0.000	0.000	0.000	0.000	0.000	0.000	0.000	0.000	0.028
K	0.000	0.000	0.000	0.000	0.000	0.000	0.000	0.000	0.000	0.000	0.000	0.000
Total cation	7.995	8.001	7.993	7.998	7.992	8.002	8.002	8.010	7.996	7.998	8.005	7.995
Fe^{3+}	0.000	0.003	0.000	0.009	0.000	0.007	0.005	0.031	0.000	0.028	0.000	0.000
XMg	0.225	0.222	0.162	0.214	0.104	0.132	0.174	0.142	0.154	0.174	0.116	0.111
Aim	0.590	0.607	0.597	0.589	0.643	0.613	0.589	0.572	0.584	0.574	0.658	0.660
Prp	0.172	0.174	0.116	0.160	0.075	0.093	0.124	0.095	0.106	0.121	0.086	0.082
Grs	0.221	0.207	0.278	0.242	0.233	0.266	0.274	0.315	0.305	0.298	0.227	0.237
Sps	0.017	0.012	0.009	0.009	0.050	0.028	0.013	0.018	0.005	0.007	0.028	0.021

(Fig. 3). X-ray image mapping of garnet 1 shown in Fig. 4 indicates the presence of an Mg-rich and Ca-poor core surrounded by an Mg-poor and Ca-rich mantle to rim before breakdown of the garnet. The outer thin rim of both garnets is similar in composition, being characterised by medium to low Ca and the highest Fe contents (Fig. 3).

4.2. Clinopyroxene

Clinopyroxene in the studied granulite occurs as a symplectitic intergrowth with plagioclase and a minor amount of orthopyroxene, hornblende, and quartz. Such symplectitic clinopyroxenes associated with plagioclase are generally observed in eclogites decompressed to granulite-facies condition (Zambezi Belt [5], Sveconorwegian Granulite Region [23], Snowbird Tectonic Zone [1], Bohemian Massif [2], and Kontum Massif [25]). These clinopyroxenes in the worldwide metamorphic terranes should contain high Na contents in high-pressure conditions, whereas they generally show augitic composition because their original jadeite components were replaced with the symplectitic sodic plagioclase. The shape of the symplectite (sometimes showing euhedral shape: Fig. 2B) in the studied granulite also suggests that the symplectite was formed from a single mineral phase, possibly corresponding to sodic clinopyroxene.

The symplectitic clinopyroxene in this study has augite composition with a few jadeite, aegyrine, and Ca-tschermak components ($Jd_{0–2}Ae_{0–3}CaTs_{0–5}$), and has a reasonably wide range of X_{Mg} values, from 0.52 to 0.59 (Fig. 5). The orthopyroxene + clinopyroxene + - plagioclase ± hornblende ± quartz symplectite was analysed using a broad probe diameter (200 μm) to obtain the original clinopyroxene composition

Table 2
Representative EDS analyses of Grt-Cpx granulite

Tableau 2
Analyses représentatives EDS de la granulite à Grt-Cpx

Mineral type	Cpx						Opx				Amp			Pl	
	Symplectite		Whole symplectite		Recalc. sympl.		Corona		Symplectite		Matrix	In Grt	Sympl.	Corona	Sympl.
SiO_2	52.75	51.64	52.28	51.37	50.18	50.84	50.05	50.40	50.72	50.12	45.19	39.27	46.08	49.17	57.18
TiO_2	0.00	0.00	0.39	0.33	0.40	0.00	0.00	0.18	0.33	0.34	0.98	0.71	1.09	0.00	0.00
Al_2O_3	1.12	0.96	7.25	8.04	7.42	6.75	0.53	0.71	0.29	0.36	9.06	16.98	8.16	32.11	27.18
Cr_2O_3	0.00	0.31	0.37	0.00	0.38	0.00	0.00	0.00	0.00	0.00	0.00	0.13	0.10	0.00	0.00
FeO	15.46	15.66	13.06	14.92	13.36	15.73	37.15	35.55	34.71	35.09	21.09	17.64	21.39	0.36	0.27
MnO	0.00	0.00	0.20	0.21	0.20	0.17	0.33	0.04	0.35	0.37	0.22	0.39	0.00	0.00	0.00
MgO	10.43	10.09	8.62	8.53	8.82	8.86	12.35	12.31	13.45	12.46	9.36	8.48	9.25	0.00	0.00
CaO	20.69	21.24	17.06	15.76	17.45	15.61	0.55	0.71	1.07	0.63	10.75	11.09	10.96	14.80	7.87
Na_2O	0.27	0.05	1.75	1.69	1.79	1.91	0.00	0.15	0.00	0.21	1.51	2.68	1.21	2.72	6.84
K_2O	0.13	0.15	0.00	0.00	0.00	0.14	0.00	0.00	0.00	0.00	0.10	0.16	0.19	0.12	0.00
Total	100.85	100.10	100.98	100.85	100.00	100.00	100.96	100.05	100.92	99.58	98.26	97.53	98.43	99.28	99.34
O	6	6	6	6	6	6	6	6	6	6	23	23	23	8	8
Si	1.997	1.981	1.932	1.910	1.888	1.921	1.984	1.998	1.989	1.998	6.807	5.939	6.924	2.261	2.574
Ti	0.000	0.000	0.011	0.009	0.011	0.000	0.000	0.005	0.010	0.010	0.111	0.081	0.123	0.000	0.000
Al	0.050	0.043	0.316	0.352	0.329	0.301	0.025	0.033	0.013	0.017	1.608	3.026	1.445	1.740	1.442
Cr	0.000	0.009	0.011	0.000	0.011	0.000	0.000	0.000	0.000	0.000	0.000	0.016	0.012	0.000	0.000
Fe	0.490	0.502	0.404	0.464	0.421	0.497	1.231	1.179	1.139	1.170	2.657	2.231	2.688	0.014	0.010
Mn	0.000	0.000	0.006	0.007	0.007	0.005	0.011	0.001	0.012	0.012	0.028	0.050	0.000	0.000	0.000
Mg	0.589	0.577	0.475	0.473	0.495	0.499	0.730	0.727	0.786	0.740	2.102	1.912	2.072	0.000	0.000
Ca	0.839	0.873	0.676	0.628	0.704	0.632	0.023	0.030	0.045	0.027	1.735	1.797	1.765	0.729	0.380
Na	0.020	0.004	0.125	0.122	0.131	0.140	0.000	0.012	0.000	0.016	0.441	0.786	0.353	0.243	0.597
K	0.006	0.007	0.000	0.000	0.000	0.007	0.000	0.000	0.000	0.000	0.019	0.031	0.036	0.007	0.000
Total cation	3.991	3.998	3.956	3.965	3.996	4.002	4.004	3.986	3.994	3.991	15.508	15.868	15.419	4.994	5.003
Fe^{3+}	0.000	0.000	0.000	0.000	0.000	0.000	0.000	0.000	0.000	0.000	1.081	0.875	0.913	–	–
XMg	0.546	0.534	0.540	0.505	0.540	0.501	0.372	0.382	0.408	0.388	0.571	0.585	0.539	–	–
An	–	–	–	–	–	–	–	–	–	–	–	–		0.745	0.389

(labelled as whole symplectite in Fig. 5) stabilised under high-pressure conditions. The results show scattered Si content [1.87 to 2.01 pfu (per formula unit); Fig. 5] and do not agree with the stoichiometries of clinopyroxene (Table 2). Most are rich in SiO_2, and their total cations are below 4.0 pfu. The compositions are similar to non-stoichiometric supersilicic clinopyroxene, as suggested in [37]. Such clinopyroxene is generally observed in ultrahigh-pressure eclogites and mostly contains quartz rods [6,15,25]. However, no such evidence is observed in the studied sample. The variety of SiO_2 content in the original clinopyroxene depends on the modal amount of quartz in the intergrowth. It could indicate that quartz in the symplectite is originally an inclusion in initial omphacitic clinopyroxene under high-pressure conditions and is not formed by breakdown of the clinopyroxene. All analyses were recalculated using the volume proportions of quartz in the areas analysed and their composition. The modal amounts were obtained by the estimation procedure reported by [25], which uses brightness levels of individual pixels in backscattered images. The amounts of quartz in broad probe analyses vary from 0.0 to 6.2 vol%. The recalculated compositions (labelled as recalculated whole symplectite in Fig. 5) are in good agreement with clinopyroxene, and the Si contents vary from 1.87 to 1.96 pfu (Fig. 5). The compositions are regarded as original clinopyroxene composition, and contain relatively high jadeite and Ca–Tschermak components ($Jd_{12–22}CaTs_{7–16}Aug_{68–80}$).

4.3. Other mineral phases

Al^{VI} contents of orthopyroxene differ depending upon their occurrences. Orthopyroxene coronas surrounding garnets show relatively high Al^{VI} contents (0.01–0.04 pfu), whereas symplectitic orthopyroxene replacing original clinopyroxene contains low Al^{VI} contents (0.00–0.02 pfu; Fig. 5).

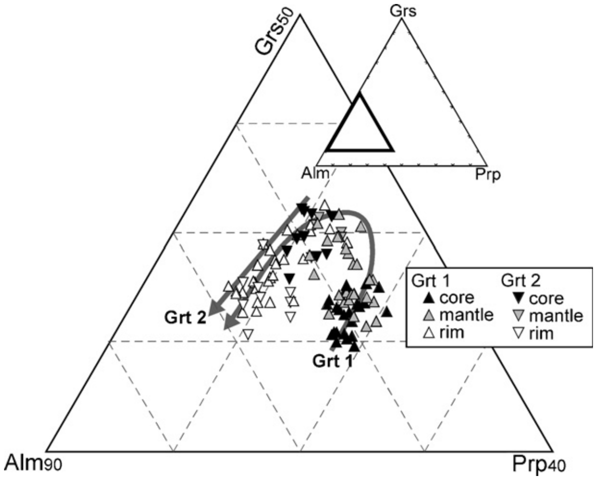

Fig. 3. Chemical composition of garnet plotted on a grossularalmandinepyrope ternary diagram. Chemical composition of garnet 1 varies from high-Mg and low-Ca to low-Mg and -Ca via high-Ca and low-Mg.

Fig. 3. Composition chimique du grenat reporté sur un diagramme ternaire grossulaire–almandin–pyrope. La composition du grenat 1 varie de haute teneur en Mg et faible teneur en Ca à faible teneur en Mg et Ca en passant par haute teneur en Ca et faible teneur en Mg.

Amphibole occurring in the matrix shows homogeneous composition (Al in T-site = 1.0–1.5 pfu, Na in M4-site = 0.2–0.4 pfu and Na + K in A-site = 0.0–0.3 pfu), indicating hornblende composition. The inclusions in garnet show low Si and high Al and Na contents (Al in T-site = 1.5–2.2 pfu, Na in M4-site = 0.2–0.3 pfu and Na + K in A-site = 0.3–0.6 pfu), characterised by pargasite to tschermakite compositions. Symplectitic hornblende replacing original clinopyroxene contains high Si and low Al and Na contents (Al in T-site = 0.8–1.4 pfu, Na in M4-site = 0.1–0.3 pfu, and Na + K in A-site = 0.0–0.2 pfu), indicating tremolitic hornblende.

Anorthite components of plagioclase coronas around garnet are much higher ($An_{60–85}$) than those of symplectitic plagioclase replacing clinopyroxene ($An_{30–50}$).

5. Monazite U Th Pb geochronology

Quantitative age determination of the garnet–clinopyroxene granulite is very difficult. Because the granulite contains neither zircons nor monazites, and

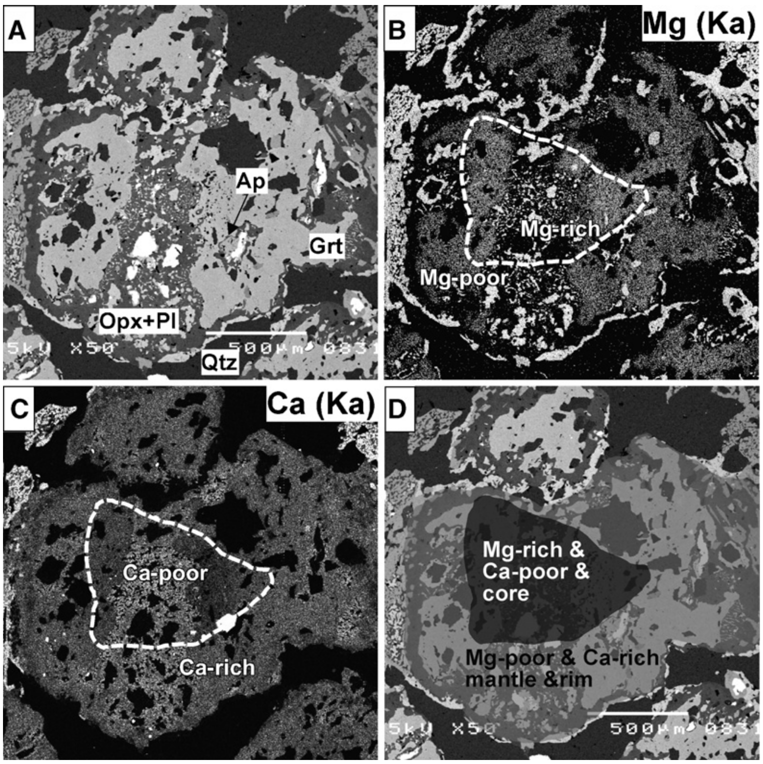

Fig. 4. Backscattered images (**A,D**) and X-ray image mappings (**B**,**C**) of huge garnet 1. The garnet should contain Mg-rich and Ca-poor core and Mg-poor and Ca-rich mantle and rim before breakdown.

Fig. 4. Images rétrodiffusées (**A**,**D**) et cartographie d'image en rayons X (**B**,**C**) de l'énorme grenat 1. Le grenat contiendrait un noyau riche en Mg et pauvre en Ca, et une enveloppe et une frange pauvre en Mg et riche en Ca avant sa dégradation.

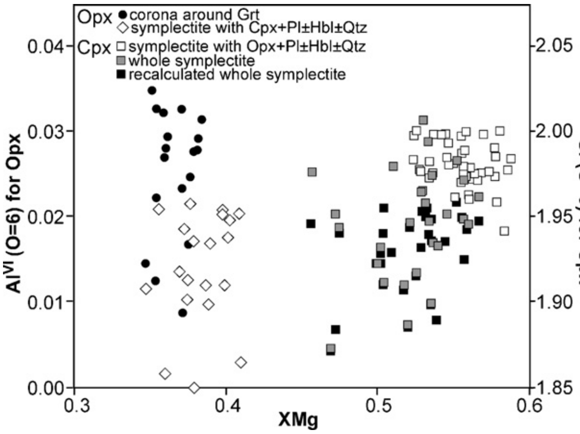

Fig. 5. Pyroxene compositions, showing X_{Mg} vs. Al or Si. The whole symplectite composition was obtained from EDS analyses using broad probe diameter. The recalculated whole symplectite composition indicates a reduced quartz component compared with whole symplectite analyses.

Fig. 5. Compositions en pyroxène montant les teneurs en X_{Mg} vs. Al ou Si. La symplectite totale été obtenue d'après des analyses EDS utilisant une sonde de grand diamètre. La symplectite totale recalculée indique une réduction de la composante quartz par rapport à la symplectite totale analysée.

because it shows complicated decompression textures formed at multiple stages, the isochron method cannot be used. Therefore, pelitic gneiss (garnet–sillimanite–biotite gneiss) from the Nam Su Lu Formation was used to obtain the metamorphic age, and monazite spot analyses were performed using a JEOL JXA-8200 microprobe analyser with four wavelength-dispersive spectrometers at the Natural Science Center for Basic Research and Development (N-BARD) in the Hiroshima University, Japan. Thin sections coated with a thin carbon film were used in the analyses. The quantitative analyses were performed with an accelerating voltage of 15 kV, a beam current of 200 nA, and a beam diameter of 5 μm using data processing by the ZAF correction program. The ThM_{α}, UM_{β} and PbM_{β} lines were measured, and other elements such as P, Y, Si, Gd, Sm, La, Ce, Pr, Nd, Ca and S were also analysed to cross-check individual data. Data corrections followed the equations suggested in [33]. Weighted means of ages were calculated using the Isoplot/Ex v.3 program [19] with 95% confidence intervals. Ward's Elk Mountain monazite (1395 Ma; [20]) was used as a consistency standard. During the analyses performed here, the average age obtained was 1396 ± 13 Ma.

The analyzed pelitic gneiss occurred with amphibolite and garnet amphibolite in the Nam Su Lu Formation. No high-pressure relicts, such as kyanite, are observed from the pelitic gneiss. It contains garnet

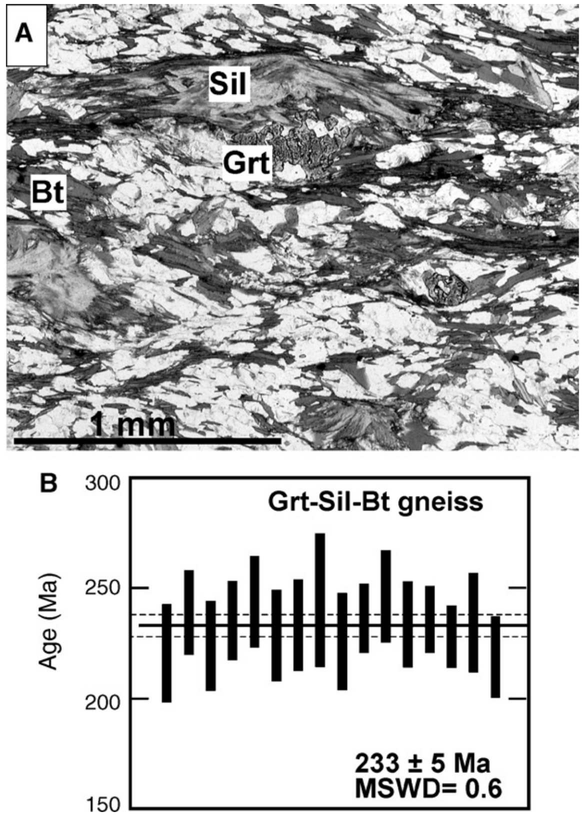

Fig. 6. Microphotographs of dated sample (**A**) and U–Th–Pb monazite ages with 2σ uncertainty (**B**). Dotted lines in **B** indicate 95% confidence intervals.

Fig. 6. Microphotographie de l'échantillon daté (**A**) et âges U–Th–Pb sur monazite, avec l'incertitude 2σ (**B**). Les lignes pointillées en **B** délimitent l'intervalle de confiance à 95 %.

porphyroblasts with biotite, sillimanite, plagioclase, K-feldspar and quartz in the matrix (Fig. 6a), indicating typical metamorphosed pelitic rock in this region. Monazite is observed as minor phases in the matrix. The ThO_2, UO_2, and PbO contents of the monazite vary from 2.757 to 7.961, 0.650 to 1.041 and 0.050 to 0.101, respectively. The apparent ages range from 220 ± 19 to 247 ± 21 Ma, indicating Early to Middle Triassic. No significant age difference was identified in all the analyses with 2 σ errors (Fig. 6). The weighted average of ages was 233 ± 5 Ma (Fig. 6).

6. Discussion and conclusions

6.1. Pressure-temperature conditions of the granulite-facies metamorphism

The petrographical and mineral chemical features suggest that sodic clinopyroxene has been stable prior to the exhumation of the granulite. The chemical

Table 3
Thermometric results of Grt-Cpx granulite

Tableau 3
Résultats de l'analyse thermométrique de la granulite à Grt-Cpx

Grt-Cpx thermometry	Mg-nch, Ca-poor Grt-recalc. Cpx	
Reference	1.5 GPa	2.0 GPa
Ellis & Green (1979)	914 °C	930 °C
Powell (1985)	902 °C	919 °C
Ravna (2000)	889 °C	922 °C
activity Jd barometry	Recalc. Cpx	
Reference temperature	800 °C	1000 °C
Holland (1983)	1.73 GPa	2.09 GPa

composition of garnet 1 drastically changes from Mg-rich and Ca-poor to Mg-poor and Ca-rich compositions (Fig. 4), indicating later external influences such as penetration of calcic melt or fluid. Hence, the high-Mg and low-Ca garnet (core of garnet 1) was stable in peak metamorphic conditions. The original sodic clinopyroxene, which is commonly stable at eclogite-facies, was probably in equilibrium with the garnet under such high-pressure/high-temperature metamorphic conditions.

The pressure/temperature conditions were estimated by garnet–clinopyroxene geothermometry [7,34,35] and activity jadeite geobarometry [12] using the core of garnet 1 and recalculating original clinopyroxene. Some recalculated original clinopyroxenes showing low Mg contents ($X_{Mg} < 0.5$) may be due to the relation to the melt (or fluid) or uncertainties of wide prove analyses, and thus they were ignored. An average value obtained from 27 recalculated clinopyroxenes ($X_{Mg} = 0.53$, X_{Jd} ($Jd/(Jd + Aug) = 0.18$) was used in this calculation. The result yielded 910–930 °C at 1.9–2.0 GPa (Table 3). Because some low-Mg clinopyroxenes were ignored in this calculation, the condition can be regarded as the minimum peak metamorphic condition for the granulite, which corresponds to high- to ultrahigh-temperature-type high-pressure granulite observed in the world [27]. After this condition, the

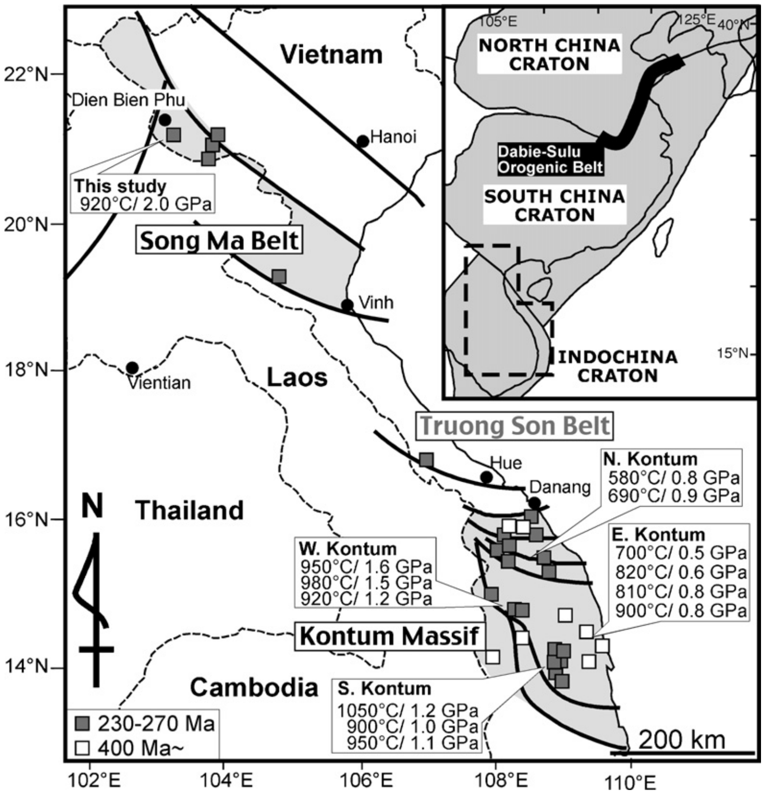

Fig. 7. Global distribution of pressure/temperature/time conditions from North to central Vietnamese metamorphic rocks. The data from the Kontum Massif are compiled from [24,26,32]. Ages from the Truong Son and Song Ma Belts are after [16]. The distribution of the Dabie Sulu Orogenic Belt is also shown in the map insert.

Fig. 7. Distribution globale des conditions pression/température/temps pour les roches métamorphiques, du Nord au Centre du Vietnam. Les données pour le massif de Kontum proviennent de la compilation de [24,26,32]. Les âges pour les chaînes de Truong Son et Song Ma proviennent de [16]. La zone orogénique de Sulu Dabie est indiquée en insertion.

granulite was uplifted and formed orthopyroxene- and plagioclase-bearing symplectites replacing sodic clinopyroxene and garnet during the decompression.

6.2. Implications for the Indochinese continental collision

High-grade metamorphic rocks including granulites and eclogites have mainly been observed in past or present plate convergence zones [21,27], and therefore, such rocks are one of the best indicators of the location of the microcontinental boundary in Asia. In the well-defined continental boundary between the North and South China cratons, such rocks have been reported: granulites from the North Dabie complex, China [39] (see inset map in Fig. 7), Imjingang belt, South Korea [36] and Higo terrane, Japan [30] and eclogites from Dabie-Sulu belt, China [8] and Gyeonggi massif, South Korea [28], some of which indicate ultrahigh-temperature [30] and ultrahigh-pressure metamorphic conditions [29]. Recently, granulites and eclogites have also been reported from the Kontum massif in central Vietnam [24–26,32] (Fig. 7). In addition, ultrahigh-temperature [24,32] and possible ultrahigh-pressure [25] conditions have been estimated from these rocks. The similarities of these rocks occurring in East to Southeast Asia are not only the metamorphic grade, but also the metamorphic age indicating the Late Permian to the Early Triassic [8,18,26,28,30,31,36] (Fig. 7). Although some older ages (~400 Ma) were also reported, their quantitative pressure/temperature conditions indicate low-pressure types (see eastern Kontum in Fig. 7), suggesting uncollisional orogeny.

The first finding of high-pressure granulites in this region strongly implies that the Song Ma Suture zone can be regarded as one of the continental boundaries between the South China and Indochina blocks. The pressure/temperature conditions (910–930 °C at 1.9–2.0 GPa) estimated from the high-pressure granulite correspond to high-temperature eclogite-facies metamorphic conditions, indicating a depth of more than 60 km. These conditions are similar to the minimum pressure conditions of eclogite overprinted by ultrahigh-temperature granulite-facies metamorphism from the Kontum massif in central Vietnam (ca. 950 °C at 1.6 GPa; [24]), though ultrahigh-pressure conditions are expected from the eclogite [25]. These rocks observed from both northern and central Vietnam commonly preserve evidence of eclogite-facies metamorphic conditions, as complicated decompression textures may indicate similar rapid exhumation from deep crustal levels. Even though we could not obtain any quantitative ages directly from the high-pressure granulite, the one of 233 ± 5 Ma, detected from pelitic gneiss, is consistent with eclogite from the Kontum massif (240 ± 16 Ma; [26]). If we assume that the age indicates a high-grade metamorphic event in northern Vietnam, these metamorphic signatures involving pressure/temperature/time conditions are quite similar to each other.

Although no evidence for granulite- and eclogite-facies metamorphism has been observed between the Song Ma Suture zone and the Kontum massif, amphibolite-facies metamorphic rocks from the Truong Son belt located between both areas have Late Permian to Early Triassic ages [16,17] (Fig. 7). In the case of the Dabie-Sulu belt (ca. 2000 km in length) in central China, well established as a continental boundary between the North and South China blocks, eclogites and granulites are only exhumed in the Dabie and Sulu areas. Therefore, in the present study, we preliminarily conclude that North to central Vietnam forms a Late Permian to Early Triassic orogenic belt (ca. 1500 km in length), due to the collision of the Indochina and South China cratons, and crustal materials subducted to deep levels are now distributed only in northern and central Vietnam (as the Song Ma metamorphic belt and the Kontum massif, respectively). Although first finding of high-pressure granulite in northern Vietnam is from a boulder sample and the age is not obtained directly from the granulite, this study strongly proposes that other evidences of the Permo-Triassic high-grade metamorphism, including eclogite and granulite, should be sought to further constrain the tectonic setting in the Indochinese collision zone.

Acknowledgements

We would like to thank Tran Ngoc Nam, P. Binh and Nguyen Tam on the field survey in Vietnam. We also acknowledge Tran Van Tri and D.D. Kiem, who gave valuable comments on the geology of the studied area. Thanks are also due to P. Agard and J.R. Kienast for critical reading of the manuscript, and to C. Lepvrier for editorial assistance. This work was partly supported by Grant-in-Aid for Scientific Research (No. 14340150 and No. 17253075: Y. Osanai) and JSPS Fellowship for Young Scientists (No. 05973: N. Nakano) from the Ministry of Education, Culture, Sports, Science and Technology, Japan.

References

[1] J.A. Baldwin, S.A. Bowring, M.L. Williams, Petrological and geochronological constrains on high pressure, high temperature

metamorphism in the Snowbird tectonic zone, Canada, J. Metamorph. Geol. 21 (2003) 81–98.

[2] H. Becker, R. Altherr, Evidence from ultra-high-pressure marble for recycling of sediments in to the mantle, Nature 358 (1992) 745–748.

[3] D.A. Carswell, Eclogite and eclogite facies: definitions and classification, in : D.A. Carswell (Ed.), Eclogite facies rocks, Chapman and Hall, New York, 1990, pp. 1–13.

[4] Department of Geology and Mineral Resources, Geology and mineral resources map of To Muong Kha-Son La sheet (F-48-XXV & F-48-XXVI), 2005.

[5] P.H.G.M. Dirks, T.A. Sithole, Eclogite in the Makuti gneiss of Zimbabwe: implications for the tectonic evolution of the Zambezi Belt in southern Africa, J. Metamorph. Geol. 17 (1999) 593–612.

[6] L. Dobrzhinetskaya, R. Schweinehage, J.J. Massonne, H.W. Green, Silica precipitates in omphacite from eclogite at Alpe Arami, Switzerland: evidence of deep subduction, J. Metamorph. Geol. 20 (2002) 481–492.

[7] D.J. Ellis, D.H. Green, An experimental study of the effect of Ca upon garnet–clinopyroxene Fe–Mg exchange equilibria, Contrib. Mineral. Petrol. 71 (1979) 13–22.

[8] W.G. Ernst, J.G. Liou, Contrasting plate-tectonic styles of the Qinling-Dabie-Sulu and Franciscan metamorphic belts, Geology 23 (1995) 353–356.

[9] D.H. Green, A.E. Ringwood, An experimental investigation of the gabbro to eclogite transformation and its petrological applications, Geochim. Cosmochim. Acta 31 (1967) 767–833.

[10] S. Hada, S. Bunopas, K. Ishii, S. Yoshikura, Rift-drift history and the amalgamation of Shan Thai and Indochina/East Malaysia blocks, in : I. Metcalfe (Ed.), Gondwana Dispersion and Asian Accretion, A.A. Balkema, Rotterdam, 1999, pp. 67–87.

[11] B. Hansen, The transition from pyroxene granulite facies to garnet clinopyroxene granulite facies. Experimental in the system $CaO–MgO–Al_2O_3–SiO_2$, Contrib. Mineral. Petrol. 76 (1981) 234–242.

[12] T.J.B. Holland, The experimental determination of activities in disordered and short-range ordered jadeitic pyroxenes, Contrib. Mineral. Petrol. 82 (1983) 214–220.

[13] C.S. Hutchison, Geological evolution of South-East Asia, Oxford Monographs on Geology and Geophysics 13 (1989).

[14] K. Ito, G.C. Kennedy, An experimental study of the basalt-garnet granulite–eclogite transition, in : J.G. Heacock (Ed.), The structure and physical properties of the Earth's crust, American Geophysical Union, Washington, D.C., 1971, pp. 303–314.

[15] I. Katayama, C.D. Parkinson, K. Okamoto, Y. Nakajima, S. Maruyama, Supersilicic clinopyroxene and silica exsolution in UHPM eclogite and pelitic gneiss from the Kokchetav massif, Kazakhstan, Am. Mineral. 85 (2000) 1368–1374.

[16] C. Lepvrier, H. Maluski, N.V. Vuong, D. Roques, V. Axente, C. Rangin, Indochina NW-trending sear zones within the Truong Son belt (Vietnam): $^{40}Ar–^{39}Ar$ Triassic ages and Cretaceous to Cenozoic overprints, Tectonophysics 283 (1997) 105–127.

[17] C. Lepvrier, H. Maluski, V.V. Tich, A. Leyreloup, P.T. Thi, N.V. Vuong, The Early Triassic Indochinian orogeny in Vietnam (Truong Son Belt and Kontum Massif); implications for the geodynamic evolution of Indochina, Tectonophysics 393 (2004) 87–118.

[18] S. Li, Y. Xiao, D. Liou, Y. Chen, N. Ge, Z. Zhang, S.-S. Sun, B. Cong, R. Zhang, S.R. Hart, S. Wang, Collision of the North China and Yangtse Block and formation of coesite-bearing eclogites: timing and processes, Chemical Geology 109 (1993) 89–111.

[19] K.R. Ludwing, Isoplot/Ex Version 3.00: a Geochronological Toolkit for Microsoft Excel, Berkeley Geochronology Center, Berkeley, CA, USA, 2003.

[20] K.H. Mahan, P. Gonçalves, M.L. Williams, J. Jercinovic, Dating metamorphic reactions and fluid flow: application to exhumation of high-P granulites in a crustal-scale shear zone, western Canadian Shield, J. Metamorph. Geol. 24 (2006) 193–217.

[21] S. Maruyama, J.G. Liou, Initiation of ultrahigh-pressure metamorphism and its significance on the Proterozoic–Phanerozoic boundary, Isl. Arc 7 (1998) 6–35.

[22] I. Metcalfe, Gondwana dispersion, Asian accretion and evolution of eastern Tethys, Aust. J. Sci. 43 (1996) 605–623.

[23] C. Möller, Sapphirine in SW Sweden: a record of Sveconorwegian (Grenvillian) late-orogenic tectonic exhumation, J. Metamorph. Geol. 17 (1999) 127–141.

[24] N. Nakano, Y. Osanai, M. Owada, T.N. Nam, T. Tsunogae, T. Toyoshima, P. Binh, Decompression process of mafic granulite from eclogite to granulite facies under ultrahigh-temperature condition in the Kontum massif, central Vietnam, J. Mineral. Petrol. Sci. 99 (2004) 242–256.

[25] N. Nakano, Y. Osanai, M. Owada, Multiple breakdown and chemical equilibrium of silicic clinopyroxene under extreme metamorphic conditions in the Kontum Massif, central Vietnam, Am. Mineral. 92(2007) 1844–1855

[26] N. Nakano, Y. Osanai, M. Owada, T.N. Nam, T. Toyoshima, P. Binh, T. Tsunogae, H. Kagami, Geologic and metamorphic evolution of the basement complexes in the Kontum Massif, central Vietnam, Gondwana Res. 12 (2007) 438–453.

[27] P.J. O'Brien, J. Rötzler, High-pressure granulites: formation, recovery of peak conditions and implication for tectonics, J. Metamorph. Geol. 21 (2003) 3–20.

[28] C.W. Oh, S.W. Kim, S.G. Choi, M. Zhai, J. Guo, K. Sajeev, First finding of eclogite facies metamorphic event in South Korea and its correlation with the Dabie-Sulu collision belt in China, J. Geol. 113 (2005) 226–232.

[29] A.I. Okey, X. Shutong, A.M. Sengör, Coesite from Dabie Shan eclogite, central China, Eur. J. Mineral. 1 (1989) 595–598.

[30] Y. Osanai, T. Hamamoto, A. Kamei, M. Owada, H. Kagami, Sapphirine-bearing granulites and related high-temperature metamorphic rocks from the Higo metamorphic terrane, west-central Kyushu, Japan, J. Metamorph. Geol. 16 (1998) 53–66.

[31] Y. Osanai, M. Owada, T. Tsunogae, T. Toyoshima, T. Hokada, T.V. Long, K. Sajeev, N. Nakano, Ultrahigh-temperature pelitic granulites from Kontum massif, central Vietnam: Evidence for East Asian juxtaposition at ca. 250 Ma, Gondwana Res. 4 (2001) 720–723.

[32] Y. Osanai, N. Nakano, M. Owada, T.N. Nam, T. Toyoshima, T. Tsunogae, P. Binh, Permo-Triassic ultrahigh-temperature metamorphism in the Kontum massif, central Vietnam, J. Mineral. Petrol. Sci. 99 (2004) 225–241.

[33] A. Pommier, A. Cocheries, O. Legendre, EPMA Dating User's Manual: Age Calculation from Electron Microanalyzer Measurements of U–Th–Pb, BRGM, Internal Report Orléans, France, 2002.

[34] R. Powell, Regression diagnostics and robust regression in geothermometer/geobarometer calibration: the garnet-clinopyroxene geothermometer revisited, J. Metamorph. Geol. 3 (1985) 231–243.

[35] E.J.K. Ravna, The garnet-clinopyroxene geothermometer – an updated calibration, J. Metamorph. Geol. 18 (2000) 211–219.
[36] J.-H. Ree, M. Cho, S.-T. Kwon, E. Nakamura, Possible eastward extension of Chinese collision belt in South Korea: The Imjingang belt, Geology 24 (1996) 1071–1074.
[37] J.R. Smyth, Cation vacancies and the crystal chemistry of breakdown reactions in kimberlitic omphacites, Am. Mineral. 65 (1980) 1185–1191.
[38] P. Tapponnier, G. Peltzer, A.Y. Le Dain, R. Armijo, Propagating extrusion tectonics in Asia: New insights from simple experiments with plasticine, Geology 10 (1982) 611–616.
[39] Y.L. Xiao, J. Hoefs, V. Den, A.M. Kerkhof, S.G. Li, Geochemical constraints of the eclogite and granulite facies metamorphism as recognized in the Raobazhai complex from North Dabie Shan, China, J. Metamorph. Geol. 19 (2001) 3–19.